



## Extracting urban vegetation characteristics using spectral mixture analysis and decision tree classifications

Thoreau Rory Tooke<sup>a,\*</sup>, Nicholas C. Coops<sup>a</sup>, Nicholas R. Goodwin<sup>a</sup>, James A. Voogt<sup>b</sup>

<sup>a</sup> Department of Forest Resource Management, 2424 Main Mall, University of British Columbia, Vancouver, Canada V6T 1Z4

<sup>b</sup> Department of Geography, 1151 Richmond St., University of Western Ontario, London, Canada N6A 5C2

### ARTICLE INFO

#### Article history:

Received 11 March 2008

Received in revised form 8 October 2008

Accepted 11 October 2008

#### Keywords:

Urban

Vegetation

High spatial resolution

Quickbird

Spectral mixture analysis

Decision tree classification

Multispectral data

### ABSTRACT

Urban vegetation cover is a critical component in urban systems modeling and recent advances in remote sensing technologies can provide detailed estimates of vegetation characteristics. In the present study we classify urban vegetation characteristics, including species and condition, using an approach based on spectral unmixing and statistically developed decision trees. This technique involves modeling the location and separability of vegetation characteristics within the spectral mixing space derived from high spatial resolution Quickbird imagery for the City of Vancouver, Canada. Abundance images, field based land cover observations and shadow estimates derived from a LiDAR (Light Detection and Ranging) surface model are applied to develop decision tree classifications to extract several urban vegetation characteristics. Our results indicate that along the vegetation-dark mixing line, tree and vegetated ground cover classes can be accurately separated (80% and 94% of variance explained respectively) and more detailed vegetation characteristics including manicured and mixed grasses and deciduous and evergreen trees can be extracted as second order hierarchical categories with variance explained ranging between 67% and 100%. Our results also suggest that the leaf-off condition of deciduous trees produce pixels with higher dark fractions resulting from branches and soils dominating the reflectance values. This research has important implications for understanding fine scale biophysical and social processes within urban environments.

© 2008 Elsevier Inc. All rights reserved.

### 1. Introduction

As our understanding of urban systems has evolved, researchers have become increasingly aware of the importance of detailed land surface characteristics to many processes established in social and physical geographic sciences. These land cover features include both natural and anthropogenic attributes and are characterized as being in a state of constant change due to the pervasive influence of human activity (Ben Dor, 2006). Urban meteorology and hydrology provide examples of disciplines which apply spatial land cover information to explain biophysical processes. Specifically, the impervious surfaces of urban areas represent an essential component of macro-scale models representing established phenomena including urban heat island effects (Oke, 1982). Spatial variation in pervious and impervious surface composition has since been demonstrated to affect surface thermal and moisture conditions; attributes that are key determinants of urban climate (Grimmond et al., 1996; Voogt & Oke, 1997).

Understanding the more complex relationships among land surface characteristics and urban climates requires that meteorolo-

gists incorporate a wide range of features beyond the basic division between impervious and pervious surfaces. Detailed land cover characteristics including surface albedo, shade, and vegetation condition inform meteorological studies at local (e.g.  $10^2$  to  $5 \times 10^4$  m) and micro- (e.g.  $10^{-2}$  to  $10^3$  m) scales (Sawaya et al., 2003; Mueller & Day, 2005). Vegetation is of particular interest as it presents a versatile resource for effectively managing and moderating a variety of problems associated with urbanization. The spatial distribution and abundance of urban vegetation, for example, is recognized as a key factor influencing numerous biophysical processes of the urban environment, including air and water quality, temperature, moisture, and precipitation regimes (Avisar, 1996; Grimmond et al., 1996; Nowak & Dwyer, 2000). Detailed vegetation characteristics, such as the structure of plant canopies and their physiological condition also exert a strong influence on more complex processes such as urban wind flow and rates of transpiration (Avisar, 1996; Wang et al., 2008). In addition, vegetated areas such as gardens, parks, and forests have been related to positive social outcomes including reductions in crime (Kuo & Sullivan, 2001), health benefits (Coen & Ross, 2006), and advanced childhood development (Taylor et al., 1998). Given the associations between vegetated land cover and the biophysical and social processes of urban systems there exists an ongoing demand for effective urban vegetation mapping and classification techniques.

\* Corresponding author. Tel.: +1 604 822 4148; fax: +1 604 822 8645.  
E-mail address: [thoreau@interchange.ubc.ca](mailto:thoreau@interchange.ubc.ca) (T.R. Tooke).

Mapping detailed land cover attributes within urban environments has been primarily reliant on conventional cadastral information from municipal agencies. However, the high cost and time consuming nature of interpreting this data, as well as difficulties in accessing data, can restrict the capacity for quantitative studies of vegetation impacts on biophysical and social processes in urban areas. In addition, cadastral information is often limited to areas of public access, resulting in large gaps of detailed land cover information across cities. In contrast, remote sensing imagery can provide information that is well suited to extensive mapping of vegetated surfaces and recent developments in high spatial resolution sensors (e.g. <math>< 5\text{ m}</math>) such as IKONOS and Quickbird have further enabled detailed analysis of urban areas. Herold et al. (2004) suggest that the visible region of the electromagnetic spectrum provides the most prominent spectral information required for separating urban land cover materials. As a result, high resolution broadband sensors with multiple channels positioned in this region of the spectrum can begin to resolve some of the detailed land cover components necessary for informing current microclimate (Noilhan & Mahfouf, 1996; Voogt & Oke, 1997) and ecological models (Zipperer et al., 1997).

Critical for the interpretation of high spatial resolution remote sensing imagery in urban environments is the development of accurate remote sensing classification techniques. Traditional supervised or unsupervised classifications assign each pixel to a single class and as a result, these classifications can significantly underestimate or overestimate land cover types in urban environments as pixels often contain a mixture of cover types. For example, research by Thomas et al. (2003) compared high resolution urban mapping methods and found that traditional supervised and unsupervised spectral classification methods resulted in map accuracies of around 50%. Urban environments also tend to contain fine scale heterogeneous land covers with narrow linear patterns (Zipperer et al., 1997; Collinge, 1998) that are not always captured within a single image pixel. Due to the inability of traditional classification algorithms to account for mixed pixels, techniques better suited to heterogeneous environments have been developed. Spectral mixture analysis (SMA), in particular, has been used to classify urban

vegetation cover (Small, 2001; Small & Lu, 2006). This approach divides pixels into representative fractions of land cover that combine at the instantaneous field of view (IFOV) of the sensor.

In the past decade SMA has developed as the primary method for extracting multiple urban land covers from a single pixel value (Kressler & Steinnocher, 1996; Small, 2001; Rashed et al., 2001). Early urban land cover classification has been theorized according to Ridd's (1995) V–I–S (vegetation–impervious surface–soil) classification scheme. This scheme provides a conceptual model that divides urban environments into three classes: vegetation, impervious surface, and soil. This approach remains problematic in a remote sensing context as it represents features that cannot necessarily be distinguished on the basis of reflectance values alone (Phinn et al., 2002; Powell et al., 2007). As a result, Small (2001) developed a more applicable model that establishes substrate, vegetation, and dark (SVD) features of the urban environment as components for SMA. These pure endmembers represent features at the apexes of the urban mixing space, yet it remains unclear whether more detailed vegetation characteristics including trees and vegetated ground cover can also be quantified in terms of their separability along the mixing line between the dark and vegetation endmembers (Small & Lu, 2006). Although higher order vegetation details including species and condition do not produce distinguishable pure pixels in three endmember mixture models, they represent physically and structurally distinct land cover features whose extraction at high spatial resolutions can inform micro- and local scale urban process models and consequently represents the central focus of the following research.

The objective of this study is to develop a technique to extract vegetation species and condition information using sub-pixel abundance values from high spatial resolution multispectral imagery. We produce fractions of vegetation, high albedo substrate, and dark features by applying spectral mixture analysis to a Quickbird image over the city of Vancouver, Canada. Shadow estimates from a LiDAR (Light Detection and Ranging) hillshade model in addition to field based observations of vegetation condition and species were collected

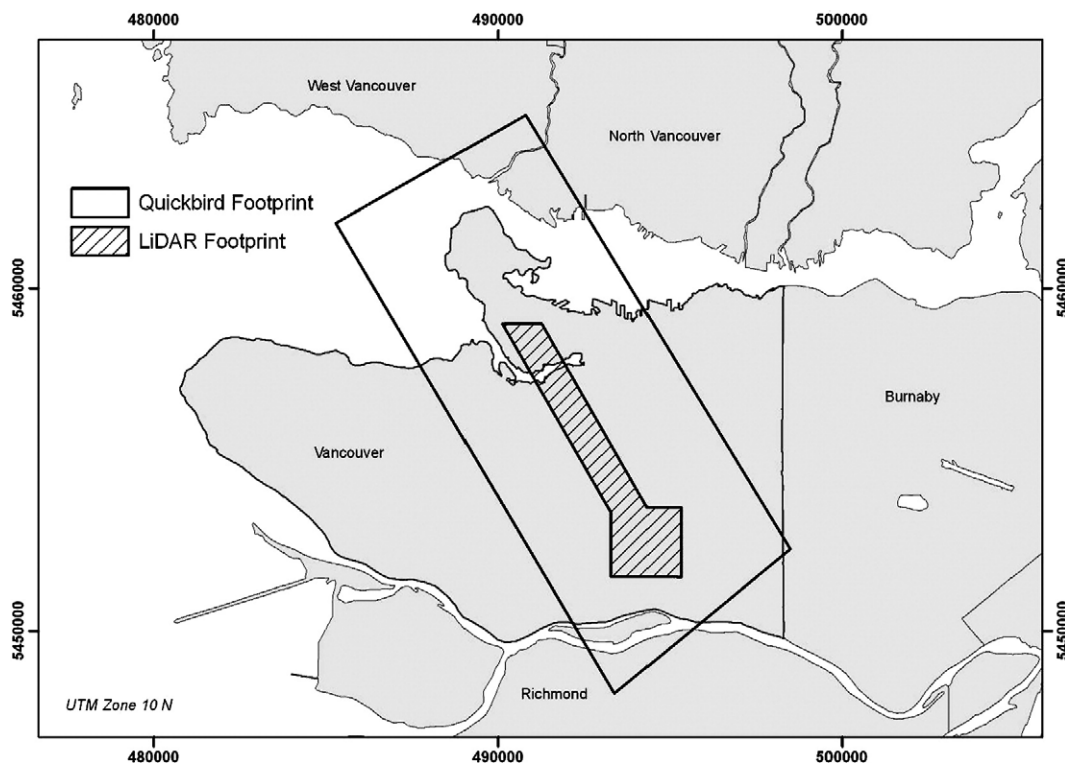


Fig. 1. Study area over Vancouver, British Columbia showing extent of Quickbird imagery and LiDAR dataset.

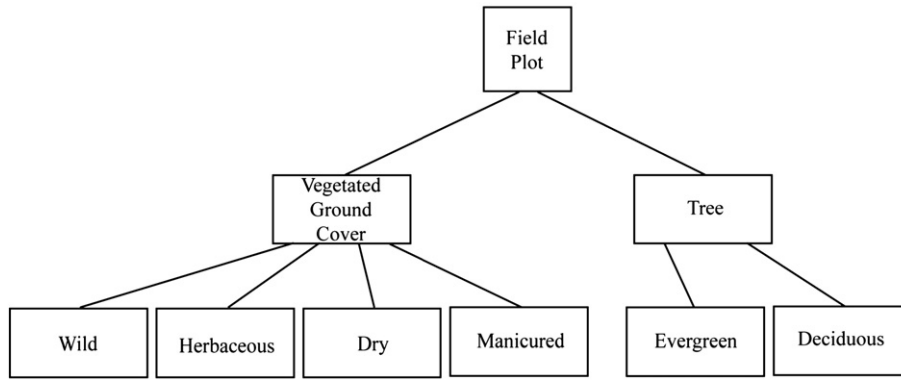


Fig. 2. Field plot classification schematic representing increasing levels of vegetation detail.

and provided training data for decision tree classifications. These parameters are used in conjunction with the SMA derived fractions of vegetation, high albedo and dark features to quantify the separability of various vegetation elements within the urban environment.

Discussion of the results focuses on issues which may impede our procedure and considerations regarding the application of this technique for modeling various fine scale urban biophysical and social processes.

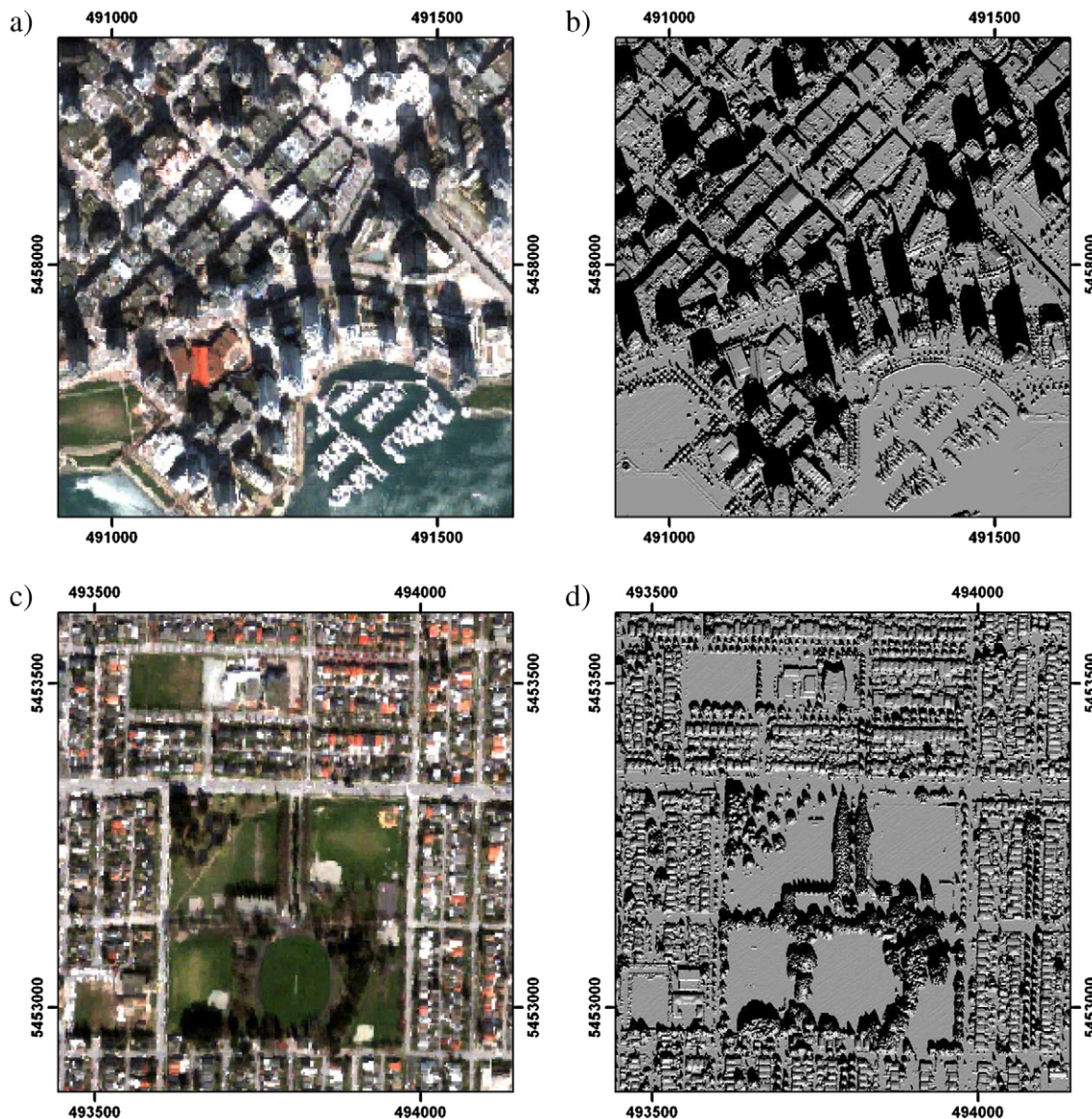


Fig. 3. Comparison between Quickbird multispectral image and LiDAR (Light Detection and Ranging) derived surface model depicting shadow for a,b) the central business district and b,c) a residential neighbourhood.

## 2. Methods

### 2.1. Study area

The City of Vancouver (49° 15'N, 123° 6'W) on the mainland western coast of Canada is located within the larger urban region of metropolitan Vancouver and covers a 114 km<sup>2</sup> area. Vegetation including various evergreen needleleaf and deciduous broadleaf tree species, shrubs, and grasses comprises a large portion of the city's surface area and due to the temperate climate of the region much of the vegetation remains green for a majority of the year (Straley, 1992). Areas of manicured grass exist throughout the city on private lots and parks, while wild native grasses are less prevalent and tend to be found in designated protected areas. Trees are also abundant throughout Vancouver with native evergreen needleleaf species dominant in urban parks and deciduous broadleaf species dominant along streets and in residential areas.

### 2.2. Remotely sensed data

A Quickbird multispectral image was acquired on March 29th 2007 over the study area, capturing a wide range of land cover types including residential, commercial, industrial, and forest (Fig. 1). The image has a spatial resolution of 2.4 m with four spectral bands (blue, 450–520 nm; green, 520–600 nm; red, 630–690 nm; and near-

infrared, 760–900 nm) and a 0.6 m panchromatic band. The Quickbird multispectral image was initially calibrated to at-sensor radiance and atmospherically corrected to estimate surface reflectance using a dark-object subtraction technique (Chavez, 1988). Digital orthorectified aerial photographs acquired in 2004 with a spatial resolution of 0.2 m were also available to provide additional land cover details.

Airborne LiDAR data was acquired in March 2007 by Terra Remote Sensing (Sidney, British Columbia, Canada) using a TRSI Mark II discrete return sensor attached to a fixed wing platform. The sensor was configured to record first and last returns with a pulse repetition frequency of 50 kHz, platform altitude of 800 m, maximum off-nadir view angle of 15°, wavelength of 1064 nm, and a fixed beam divergence angle of 0.5 mrad. The average pulse spacing equalled one laser pulse return per 0.7 m<sup>2</sup>. Ground and non-ground returns were classified using TerraScan software (Terrasolid, Finland). The area surveyed includes a 1 km wide and 9 km long transect from Stanley Park, through downtown Vancouver which contains a large number of high rise buildings, to a research observation tower located in a residential area (Fig. 1).

### 2.3. Field data

In our analysis detailed vegetation characteristics including condition and species were recorded to provide the necessary training

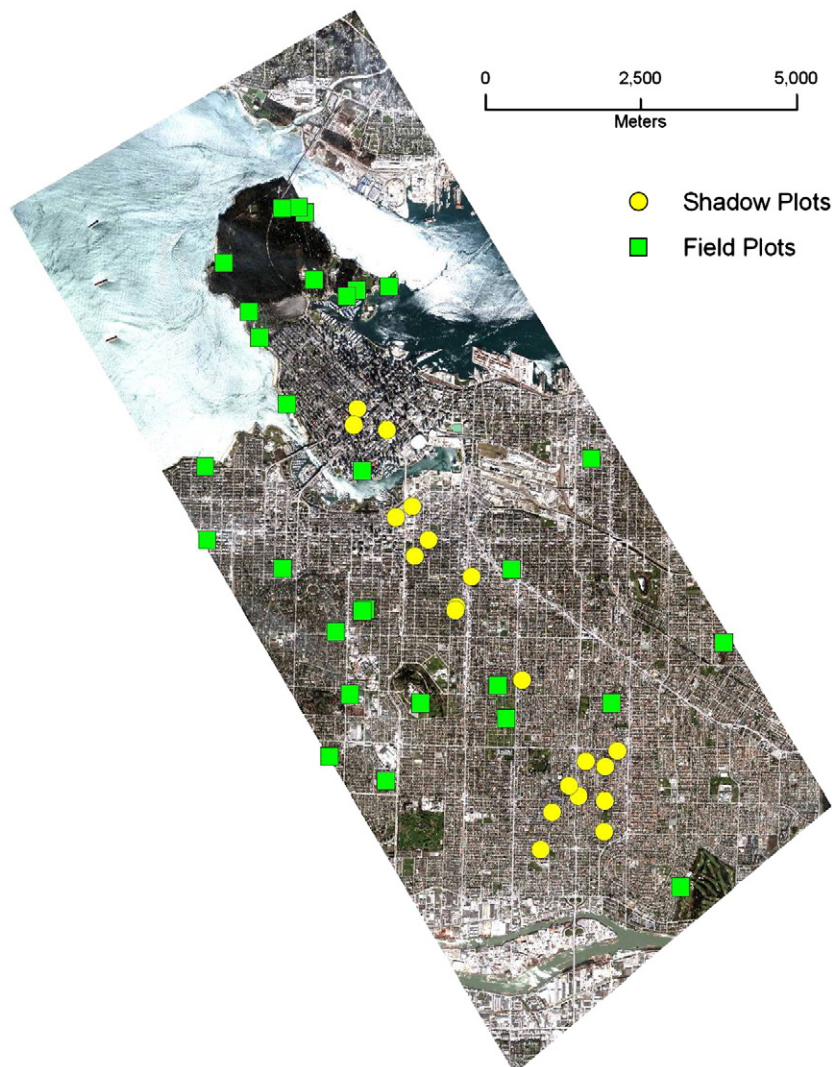


Fig. 4. Location of the field plots and shadow plots within the spatial extent of the Quickbird imagery.

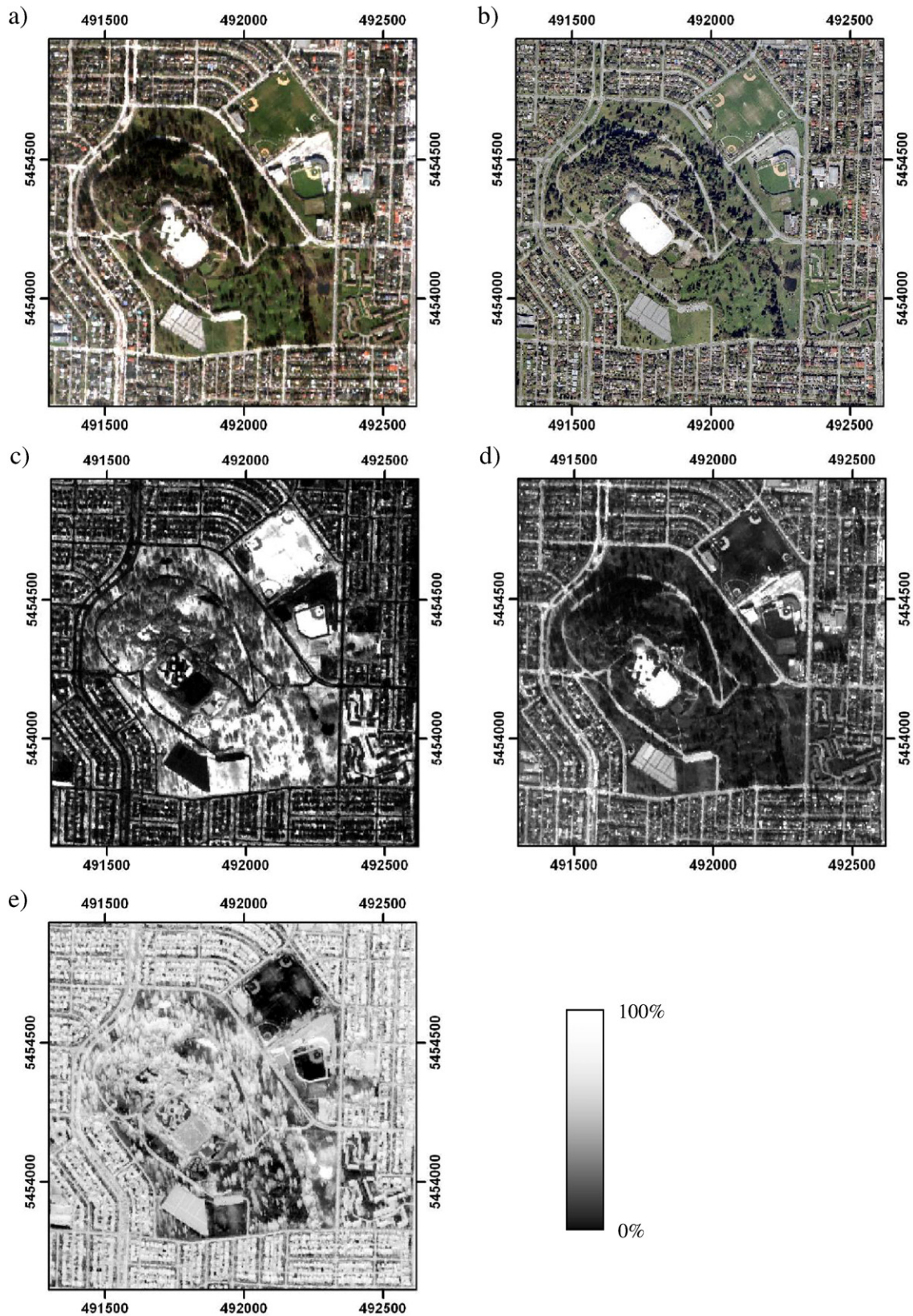


Fig. 5. True colour a) multispectral Quickbird image and b) aerial photograph compared with image fractions for the three endmembers: c) vegetation, d) high albedo substrate, and e) dark.

data for decision tree classifications of urban vegetation. Fig. 2 displays a list of the vegetation characteristics recorded in the field to investigate the location of these features within the mixing space of

high resolution satellite imagery particular to the City of Vancouver. Vegetation is separated into tree and vegetated ground cover categories, and then each category is further classified based on the

species and condition of the vegetation. The vegetated ground cover class is separated into wild (unmanicured and long grasses), herbaceous plants, dry grasses (senesced and dead), and manicured grasses. The tree class is separated according to whether the vegetation is a deciduous broadleaf or evergreen needleleaf species.

#### 2.4. Field plots

Field locations were selected to capture a wide range of vegetation patterns, condition and species. Due the significant areas of private land uses in the urban setting sites were chosen in areas with minimal limitations to access and as a result most of the field plots were located in public spaces. Accessibility was evaluated using orthophotographs, street maps, and a *a priori* knowledge of the region. Navigation to the field plots was done using a differential GPS unit applying wide area augmentation system (WAAS) technology and orthophotographs. The extreme heterogeneity of urban environments compared to natural landscapes provides new challenges when attempting to validate the results of high resolution imagery to field based observations. Because numerous contrasting surfaces are being analyzed according to their influence on the spectral response of a pixel or group of pixels, it is critical that the field plots representing those portions of the image align with sub-pixel accuracy. To address this issue imagery was referenced using spatial subsets from the orthophotographs and rectified to a pansharpened Quickbird image with RMS errors less than 1 m.

#### 2.5. Shaded area estimation using LiDAR data

To identify image pixels representing shadow a hillshade model was developed using a LiDAR transect overlapping the center of the Quickbird scene. First return heights were gridded with  $1 \times 1$  m pixels to represent the maximum height/urban vertical profile across the study area. Using collection date specifications from the Quickbird imagery and a hillshade model the incoming solar radiation was estimated. Input parameters consisted of a sun zenith angle of  $43.5^\circ$  and azimuth orientation of  $167.1^\circ$ . The resulting model and multi-spectral Quickbird image are shown in Fig. 3.

#### 2.6. Linear spectral mixture analysis

SMA divides each pixel of an image into the representative fraction of selected endmember spectra. Each endmember consists of spectra that represent materials on the ground (Adams & Gillespie, 2006). Linear mixing assumes that the spectral reflectance profile of each pixel is a linear combination of the selected endmembers (Goodwin et al., 2005). To find the best combination of endmembers to explain the mixed reflectance signal of a pixel, matrix inversion is performed by Eq. (1).

$$R_i = \sum_{j=1}^n f_j RE_{ij} + \varepsilon_i \text{ and } 0 \leq \sum_{j=1}^n f_j \leq 1 \quad (1)$$

where  $R_i$  is the total pixel reflectance;  $f_j$ , the endmember image fraction;  $RE_{ij}$ , the reflectance of image endmember  $j$  at band  $i$ ;  $n$ , the number of endmembers; and  $\varepsilon_i$  is the residual error for band  $i$ . The number of possible endmembers equals the number of bands minus 1.

Our spectral mixture analysis procedure is performed following the methods presented by Small and Lu (2006). The first step involves a principle components (PC) analysis on the four bands of the Quickbird image. Performing PC transformations on broadband imagery enables the topology of the mixing space to be constructed as a three dimensional model which encompasses all the combinations of theoretically pure physical elements within each pixel of the scene (Small & Lu, 2006). These pure features, referred to as endmembers, compose the apexes of the three dimensional mixing

space (modeled as a convex hull) and must be carefully selected to ensure that accurate mixture models are produced. To maintain the integrity of the analysis pixels are manually selected from the apexes of the mixing space and verified against georeferenced orthophotos. Similar to previous research (Rashed et al., 2001; Small, 2001; Small & Lu, 2006) the endmembers were defined as vegetation, high albedo substrate, and dark features. Dark endmember pixels include shadows typically cast by tall buildings in the central business district of the city, in addition to significant areas of shadowed forest canopies in evergreen needleleaf forests. Vegetation endmember pixels are characterized as highly manicured grasses typically located in golf courses and public parks. The final step in the analysis uses Eq. (1) to perform SMA and generate three abundance images representing each of the individual endmembers. To produce abundance images with meaningful values that can be coupled with field observations sum to unity and positivity constraints are applied to the analysis and fractions represented as a percentage.

#### 2.7. Decision tree classification

Decision trees (DTs) have emerged recently as an alternative land cover classification method and may provide improved accuracies over maximum likelihood and neural network classifications when applied to multispectral imagery (Mahesh & Mather, 2003). DTs offer advantages over these other types of classification methods in that they can process data measured at different scales and no assumptions are made concerning the frequency distributions of the data. In addition DTs are relatively quick; requiring minimal computational time compared to neural networks (Mahesh & Mather, 2003). The basic process of DT construction involves the repeated division of a set of training data into increasingly distinct subsets based on tests to one or more of the feature values. Once a set of hierarchically structured rules, or branches, are produced based on the provided training data, then these rules can be applied to an entire image in order to produce accurate land cover maps and inventories for further spatial analysis.

In our analysis, the training data are derived from the field based observations of vegetation species and condition in addition to the LiDAR derived shadow plots (Fig. 4). Single trees for each hierarchical level of vegetation class are developed in DTREG using a 10 V-fold cross validation technique which has been demonstrated to produce highly accurate results without requiring an independent dataset for assessing the accuracy of the model (Sherrod, 2008). A more detailed explanation of decision tree validation and pruning techniques can be found in Sherrod (2008). The V-fold cross validation technique used in this paper involves first developing an initial large tree using all the available data, known as the reference tree. Secondly the total dataset is partitioned into 10 groups (or folds) and 10 new subsets of the total are created using 9 out of 10 of the folds. Ten test trees are then built

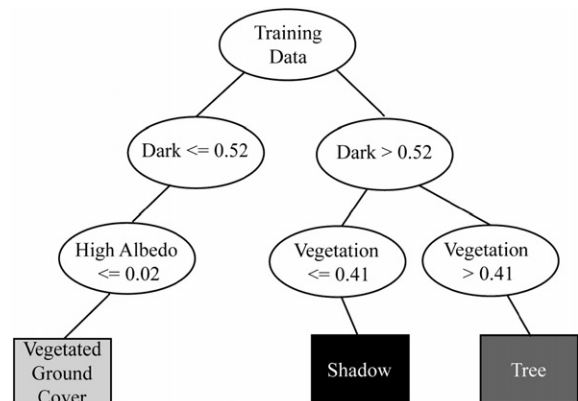


Fig. 6. Statistically developed decision tree classification for the extraction of broad level vegetation characteristics including trees and vegetated ground cover.

using the reduced datasets with the unused 10% in each case then run through each test tree and the classification error for that tree computed. Once the 10 test trees have been built, their classification error rate as a function of tree size is averaged and the reference tree is pruned to the number of nodes matching the size that produces the minimum cross validation cost (Breiman et al., 1984).

### 3. Results

The principal component analysis on the 4 band Quickbird image showed over 99% of the image variance contained within the first three primary principal components, which is in agreement with earlier research (Small, 2003; Small & Lu, 2006). The resulting distribution of pixel values within the mixing space produced distinctive linear dispersions between the vegetation-dark and dark-high albedo apexes, while a concave dispersion was observed between

the vegetation-high albedo apexes indicating that few pure binary mixtures of these features exist within the city (Small & Lu, 2006).

The abundance images produced from the SMA for the vegetation, high albedo substrate and dark features of the imagery in addition to the true colour multispectral Quickbird and orthophoto images is shown in Fig. 5. The dark abundance image shows the dominance of dark features throughout the scene resulting from significant shadowing which comprises this endmember. Comparing the areas of vegetation in the orthophotograph (Fig. 5) with the corresponding dark and vegetation abundance images also indicates that certain forms of vegetation are underestimated in a three endmember mixing model, specifically trees which have moderate fractions of both dark and vegetation features. High fractions displayed in the vegetation abundance image are localized in grassy areas, while surfaces including roads and parking lots are highlighted in the representative high albedo substrate image.

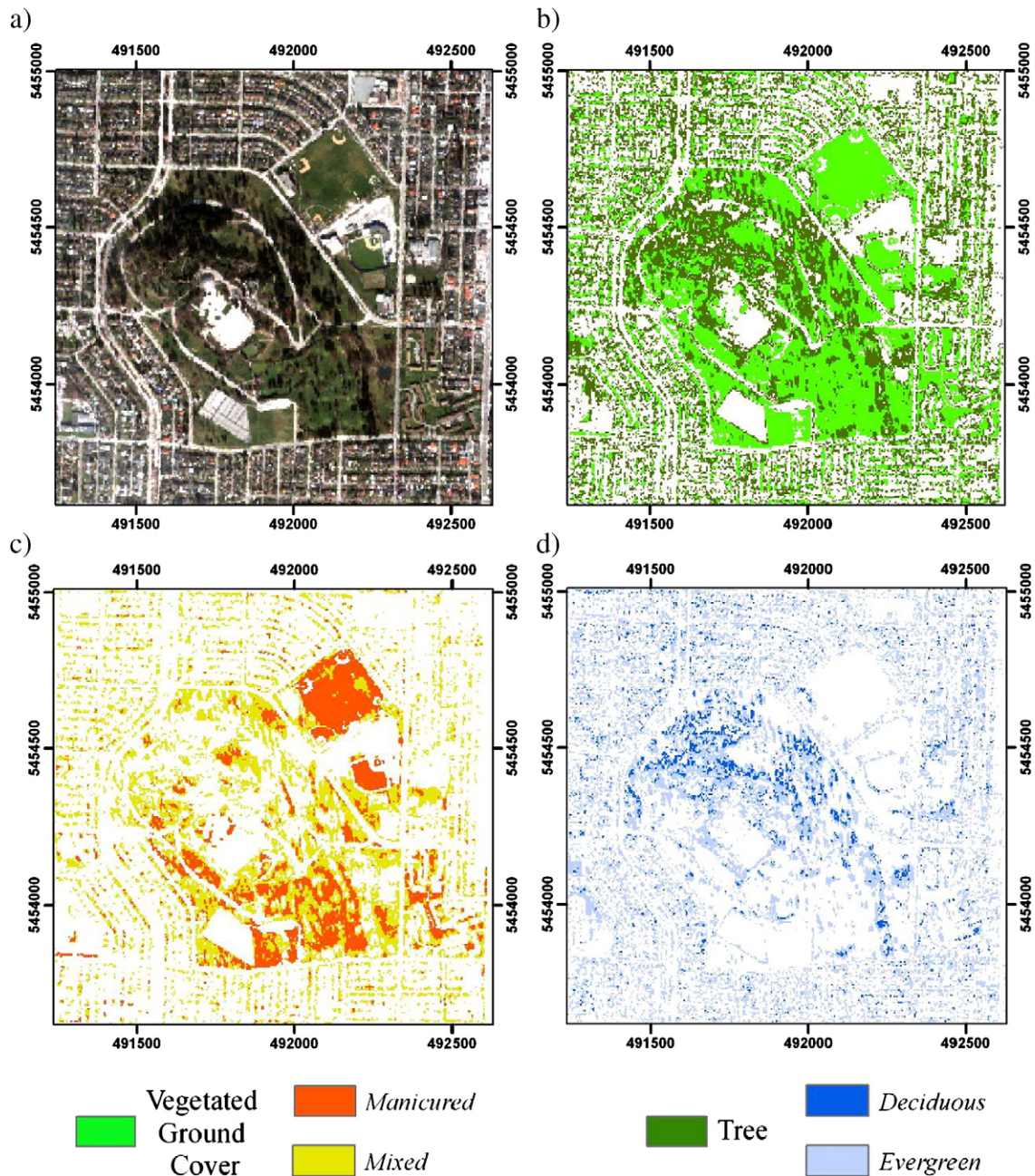
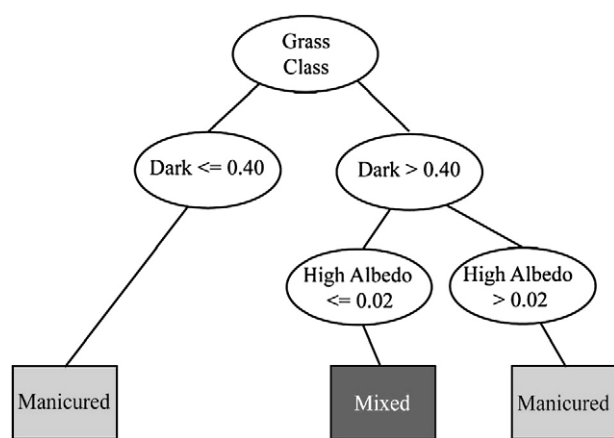


Fig. 7. Mapped decision tree results comparing a) the true colour multispectral Quickbird image with extracted b) grass and vegetated ground cover classes, c) manicured and mixed grass classes, and d) deciduous and evergreen tree species classes.



**Fig. 8.** Statistically developed decision tree classification for the extraction of detailed second order vegetation characteristics related to vegetated ground cover condition including: manicured and mixed.

To determine the location and separability of various vegetation features within the image mixing space, field observations were collected with classes representing hierarchical levels of vegetation detail. The first order represents vegetated ground cover and trees and the second order represents species and condition attributes related to the vegetation. Data collected for each hierarchical level were used as input into decision tree classification models and determined which categories or combination of categories could be separated and successfully classified within the decision tree models. A total of three decision trees were successfully produced, the first representing broad divisions of vegetation (vegetated ground cover and tree) and the second two representing more detailed vegetation classes as subsets of the broader categories (manicured, mixed, evergreen, and deciduous).

The first model representing the first level of vegetation detail explained 94% of the variance within the vegetated ground cover class and 80% of the variance within the tree class. The primary factor for dividing these two classes is the dark abundance image (Fig. 6). The first split involved separating the dark values at 52%. Pixels with less than 52% dark features were then classified into vegetated ground cover pixels with a further rule applying high albedo abundance values of greater than 2%. Dark values greater than 52% include both shadow and tree classes and these image features were separated using the vegetation abundance with a threshold of 41% where pixels less than this value were classified as shadow and values greater than 41% were classified as tree. Results from this classification are mapped in Fig. 7b.

Successful extraction of the first order vegetation classes enabled the application of our decision tree technique for extracting the more detailed second order classes. Pixels classified as vegetated ground cover from the previous step were input into a new DT to extract the classes of manicured, dry, herbaceous and wild. The best result involved combining dry, wild, and herbaceous categories into a new class labelled 'mixed', while the manicured class remained unchanged from the original data. This classification used the dark abundance values as the primary feature for classification (Fig. 8). The first rule establishes a threshold of 40% dark and all pixels less than this value were classified as manicured grass. An additional rule was required to separate the remaining classes and used the high albedo abundance value of 2% to derived mixed grasses (less than 2%) and the remaining manicured grass class (greater than 2%). Variance explained for this DT classification was 100% for the manicured class and 73% for the mixed grass class (mapped in Fig. 7c).

The final classification extracted evergreen and deciduous classes from the broader tree category. This classification used the dark abundance values as the first feature for classification (Fig. 9). The only branch in this DT establishes a threshold of 57% dark with tree pixels

less than this value classified as evergreen and pixel greater than 57% dark classified as deciduous. Variance explained for this DT classification was 80% for the evergreen class and 67% for the deciduous class (mapped in Fig. 7d).

## 4. Discussion

### 4.1. Vegetation separability

Mapping the location and spatial extent of trees, vegetated ground cover, and high level vegetation detail provides a valuable addition to urban land cover mapping using high spatial resolution imagery. Image classification techniques developed to date extract a basic vegetation class which encompasses a broad range of features whose structural and spectral diversity have a variety of impacts on urban processes (Mueller & Day, 2005; Voogt & Oke, 1997). Spectral mixture analysis provides a successful technique for extracting the fractional abundance of general land cover features well suited to the heterogenic composition of urban environments. Small and Lu (2006) explain that high spatial resolution image vegetation fractions provide more informative vegetation estimates than moderate resolution imagery due to the reduction of possible distinct mixtures and add that Quickbird pixels can resolve many of the individual components representing urban vegetation. Nonetheless, the dimensionality of the imagery still produces a three endmember mixture model encompassing various vegetation conditions and species. Fractional abundance values (Fig. 5) from our analysis show that vegetation is generally represented by manicured grasses and as a result underestimates the spatial extent of trees within the mixing space.

To improve the classification of vegetation features and explain the endmember variability within high spatial resolution mixing space, we applied a decision tree classification using field observations and the SMA derived abundance images. Of significance, this enabled accurate estimates of the separability and location of vegetation features including tree species and vegetated ground cover condition within the mixing space.

Several hierarchical orders of classes were established with increasing levels of detail regarding vegetation condition and species. The first order classification involved separating trees from vegetated ground cover. As the results indicate, this procedure explains 94% of the variance for the vegetated ground cover class and 80% of the variance for the tree class. The spectral distinction between these two vegetation categories is largely a result of structural differences. Vegetated ground cover tends to be close to the ground with closely-spaced foliage resulting in little shadowing, enabling a strong reflectance of photosynthetically active vegetation back to the sensor. Alternatively, the horizontal variation in vertical structure of trees causes significant shadowing interspersed throughout the foliage. These structural differences result in varying amounts of shadow

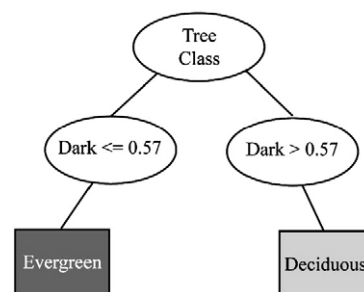


**Fig. 9.** Statistically developed decision tree classification for the extraction of detailed second order vegetation characteristics related to tree species including: deciduous broadleaf and evergreen needleleaf.

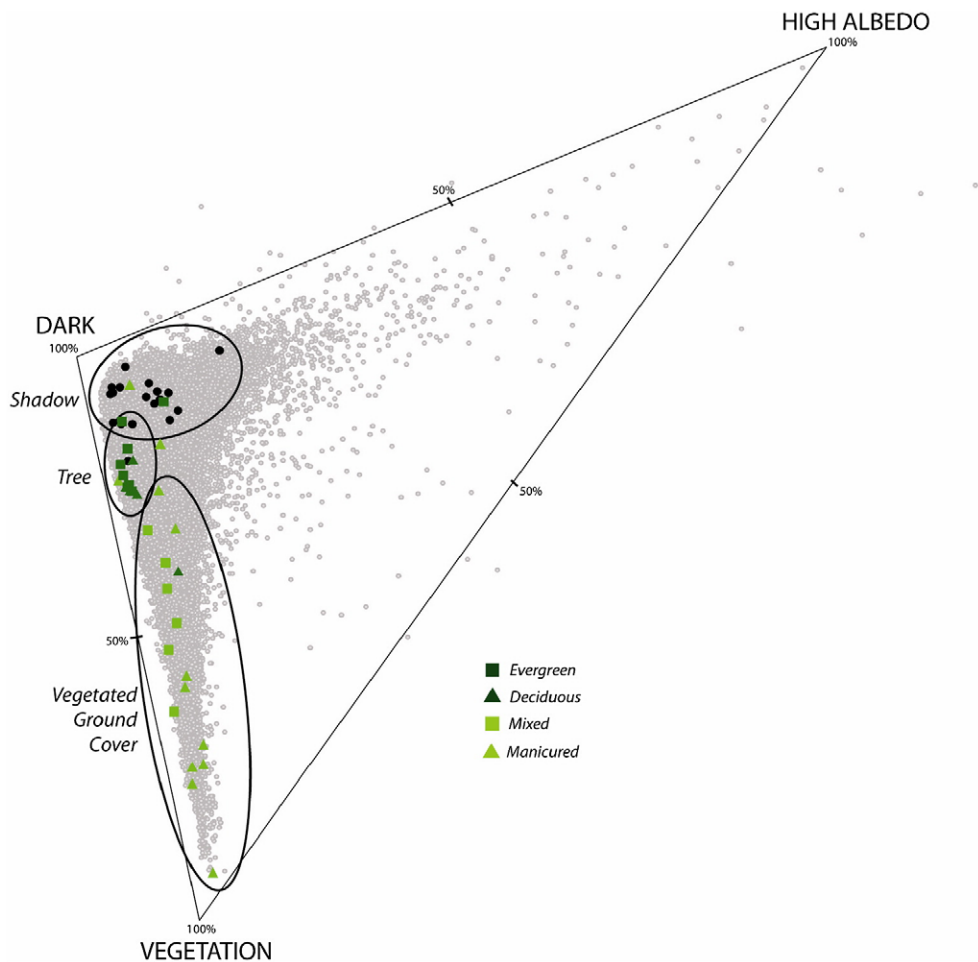


**Fig. 10.** Model depicting where shadow and vegetation characteristics including trees and vegetated ground cover and associated condition and species locate within the three endmember mixing space of a high spatial resolution spring image over Vancouver.

captured within a Quickbird pixel which are extracted in the 'dark' branch of the DT model in Fig. 6. As a result of greater shadowing, trees are separable from vegetated ground cover in the mixing space and are localized closer towards the apex of the dark endmember along the vegetation-dark mixing line.

After the successful extraction of the general vegetation classes of vegetated ground cover and tree, the same technique was applied to provide estimates of more detailed characteristics including species and condition. Several important discussion points are raised as a result of the analysis. Separating evergreen needleleaf and deciduous broadleaf trees using our technique explained 80% and 67% of the variance respectively. Deciduous trees have significant variations in leaf characteristics in terms of shape, size, and pigment compared with many evergreen species. In addition, the Quickbird image was captured in spring when the spectral response of deciduous broadleaf trees is strongly affected by the seasonal variability associated with tree phenology (many deciduous species are beginning to bud in Vancouver). We suggest that the leaf-off condition of deciduous trees results in the counterintuitive decision tree shown in Fig. 8 where pixels with higher dark fractions are classified as 'deciduous' resulting from branches and soils dominating the reflectance values associated with deciduous tree species.

Fig. 10 displays a model based on the DT classifications indicating how various levels of vegetation features localize within the mixing space. This model is image specific and, in this case, represents the location of vegetation features during the spring season. Future work may be undertaken to study the seasonal variation of feature location

and separability within the mixing space, and might also benefit from quantifying the location of higher level mixing spaces within the original three endmember model. Seasonal selection of high resolution imagery is an important consideration which will vary the location and separability of vegetation features. Selecting a spring image for our analysis provided good separability of vegetated ground cover and trees and associated condition and species details.

#### 4.2. Applications

Mapping and modelling tree and vegetated ground cover characteristics from high spatial resolution satellite imagery in urban areas enables significant advancements in our understanding of urban systems. Boundary-layer climates are significantly influenced by the distribution, abundance, condition and characteristics of urban vegetated surfaces at local and micro-scales (Voogt & Oke, 1997). Imagery representing vegetation dynamics across urban areas can provide urban planners with vital information required to mitigate heat island effects and reduce building energy requirements associated with heating and cooling (Grimmond, 2007). At the same time, vegetation characteristics across a city can inform epidemiologists of the spatial distribution of health risks related to urban air quality (Corburn, 2007). Separating vegetation into more detailed classes also has strong potential to inform urban ecologists of species occurrence and vulnerable plant, animal, and bird habitats associated with urban vegetation cover and its spatial pattern across the landscape (Zipperer et al., 1997).

## 5. Conclusion

Refining our understanding of urban systems through accurate vegetation mapping is critical to the wellbeing of urban residents and the sustainability of our cities. This paper examined the abundance of urban endmembers in a Quickbird image over the City of Vancouver and applied decision tree classifications to quantify and separate various orders of vegetation detail. Results demonstrate successful extraction of trees and vegetated ground cover using our technique. This technique also proved successful in extracting vegetation species and condition including evergreen needleleaf, deciduous broadleaf, manicured and mixed grass, and highlights the phenological impacts of more detailed vegetation features on the separability of species and condition classes within the mixing space. Our analysis provides an operational technique to enable vegetation extraction and related studies across a variety of urban areas and will help parameterize models related to urban biophysical processes. Further research will involve the collection of summer imagery and a comparison of the accuracy at which the vegetation classes can be extracted compared to this current analysis.

## Acknowledgments

This research was supported by the Environmental Prediction in Canadian Cities (EPiCC) project funded by the Canadian Foundation for Climate and Atmospheric Sciences (CFCAS). The authors would like to thank field assistants Brad Lehrbass, Colin Ferster, Sam Coggins, and Trevor Jones as well as Sue Grimmond, Jinfei Wang, and Timothy Oke for their insight into remote sensing considerations for urban micrometeorological applications. We would also like to thank Christopher Small and two anonymous reviewers for their helpful critiques and comments.

## References

- Adams, J. B., & Gillespie, A. R. (2006). *Remote sensing of landscapes with spectral images: A physical modeling approach*. New York: Columbia University Press.
- Avissar, R. (1996). Potential effects of vegetation on the urban thermal environment. *Atmospheric Environment*, 30(3), 437–448.
- Ben Dor, E. (2006). Imaging spectrometry for urban applications. In F. D. van Meer, & S. M. de Jong (Eds.), *Imaging Spectrometry* (pp. 243–281). Dordrecht: The Netherlands: Springer.
- Breiman, L., Friedman, J., Olshen, R., & Stone, C. (1984). *Classification and Regression Trees*. Belmont, CA: Wadsworth International Group.
- Chavez, P. S., Jr. (1988). An improved dark-object subtraction technique for atmospheric scattering correction of multispectral data. *Remote Sensing of Environment*, 24, 459–479.
- Coen, S. E., & Ross, N. A. (2006). Exploring the material basis for health: Characteristics of parks in Montreal neighbourhoods with contrasting health outcomes. *Health and Place*, 12, 361–371.
- Collinge, S. K. (1998). Spatial arrangement of habitat patches and corridors: Clues from ecological field experiments. *Landscape and Urban Planning*, 42, 157–168.
- Corburn, J. (2007). Urban land use, air toxics and public health: Assessing hazardous exposures at the neighbourhood scale. *Environmental Impact Assessment Review*, 27(2), 145–160.
- Goodwin, N., Coops, N., & Stone, C. (2005). Assessing plantation canopy condition from airborne imagery using spectral mixture analysis and fractional abundances. *International Journal of Applied Earth Observation and Geoinformation*, 7, 11–28.
- Grimmond, S. (2007). Urbanization and global environmental change: Local effects of urban warming. *Geographical Journal*, 173, 83–88.
- Grimmond, C. S. B., Souch, C., & Hubble, M. D. (1996). The influence of tree cover on summertime energy balance fluxes, San Gabriel Valley, Los Angeles. *Climate Research*, 6, 45–57.
- Herold, M., Roberts, D. A., Gardner, M. E., & Dennison, P. E. (2004). Spectrometry for urban area remote sensing — development and analysis of a spectral library from 350 to 2400 nm. *Remote Sensing of Environment*, 91, 304–319.
- Kresler, F., & Steinnocher, K. (1996). Change detection in urban areas using satellite images and spectral mixture analysis. *International Archives of Photogrammetry and Remote Sensing*, 31, 379–383.
- Kuo, F. E., & Sullivan, W. C. (2001). Environment and crime in the inner city. *Environment and Behavior*, 33(3), 343–365.
- Mahesh, P., & Mather, P. M. (2003). An assessment of the effectiveness of decision tree methods for land cover classification. *Remote Sensing of Environment*, 86, 554–565.
- Mueller, E. C., & Day, T. A. (2005). The effect of urban ground cover on microclimate, growth and leaf gas exchange of oleander in Phoenix, Arizona. *International Journal of Biometeorology*, 49(4), 244–255.
- Noilhan, J., & Mahfouf, J. F. (1996). The ISBA land surface parameterisation scheme. *Global and Planetary Change*, 13, 145–149.
- Nowak, D. J., & Dwyer, J. F. (2000). The Urban Forest Effects (UFORE) Model: Quantifying urban forest structure and functions. In M. Hansen, & T. Burk (Eds.), *Proceedings: Integrated tools for natural resources inventories in the 21st century. IUFRO Conference, 16–20 August 1998, Boise, ID. General Technical Report NC-212, U.S. Department of Agriculture, Forest Service, North Central Research Station, St. Paul, MN* (pp. 714–720).
- Oke, T. R. (1982). The energetic basis of the urban heat island. *Quarterly Journal of the Royal Meteorological Society*, 108, 1–24.
- Phinn, S., Stanford, M., Scarth, P., Murray, A. T., & Shyy, P. T. (2002). Monitoring the composition of urban environments based on the vegetation–impervious surface–soil (VIS) model by subpixel analysis techniques. *International Journal of Remote Sensing*, 23(20), 4131–4153.
- Powell, R. L., Roberts, D. A., Dennison, P. E., & Hess, L. L. (2007). Sub-pixel mapping of urban land cover using multiple endmember spectral mixture analysis: Manaus, Brazil. *Remote Sensing of Environment*, 106, 253–267.
- Rashed, T., Weeks, J. R., Gadalla, M. S., & Hill, A. G. (2001). Revealing the anatomy of cities through spectral mixture analysis of multispectral satellite imagery: A case study of the greater Cairo region, Egypt. *Geocarto International*, 16(4), 7–17.
- Ridd, M. K. (1995). Exploring a V–I–S (vegetation–impervious surface–soil) model for urban ecosystem analysis through remote sensing: Comparative anatomy for cities. *International Journal of Remote Sensing*, 16, 2165–2185.
- Sawaya, K. E., Olmanson, L. G., Heinert, N. J., Brezonik, P. L., & Bauer, M. E. (2003). Extending satellite remote sensing to local scales: Land and water resource monitoring using high-resolution imagery. *Remote Sensing of Environment*, 88, 144–156.
- Sherrod, P. H. (2008). *DTREG Predictive Modeling Software. Users Manual. www.dtreg.com/DTREG.pdf*
- Small, C. (2001). Estimation of urban vegetation abundance by spectral mixture analysis. *International Journal of Remote Sensing*, 22(7), 1305–1334.
- Small, C. (2003). High spatial resolution spectral mixture analysis of urban reflectance. *Remote Sensing of Environment*, 88, 170–186.
- Small, C., & Lu, J. W. T. (2006). Estimation and vicarious validation of urban vegetation abundance by spectral mixture analysis. *Remote Sensing of Environment*, 100, 441–456.
- Straley, G. B. (1992). *Trees of Vancouver*. Vancouver: UBC Press.
- Taylor, A. F., Wiley, A., Kuo, F. E., & Sullivan, W. C. (1998). Green spaces as places to grow. *Environment and Behavior*, 30(1), 3–28.
- Thomas, N., Hendrix, C., & Congalton, R. G. (2003). A comparison of urban mapping methods using high-resolution digital imagery. *Photogrammetric Engineering and Remote Sensing*, 69(9), 963–972.
- Voegt, J. A., & Oke, T. R. (1997). Complete urban surface temperatures. *Journal of Applied Meteorology*, 36, 1117–1132.
- Wang, J., Endreny, T. A., & Nowak, D. J. (2008). Mechanistic simulation of tree effects in an urban water balance model. *Journal of the American Water Resources Association*, 44(1), 75–85.
- Zipperer, W. C., Sisinni, S. M., & Pouyat, R. V. (1997). Urban tree cover: An ecological perspective. *Urban Ecosystems*, 1, 229–246.